Fracture Mechanics of Concrete and Concrete Structures - High Performance, Fiber Reinforced Concrete, Special Loadings and Structural Applications- B. H. Oh, et al. (eds)

Identification of the stress-crack opening behavior of HPFRCC: the role of flow-induced fiber orientation

L. Ferrara, M. di Prisco & M.G.L. Lamperti
Department of Structural Engineering, Politecnico di Milano, Italy

ABSTRACT: a High Performance Fiber Reinforced Cementitious Composite (HPFRCC), containing 100 kg/m^3 straight steel fibers (l_f = 13 mm; d_f = 0.16 mm), has been designed for precast roof elements and thin slabs where fibers act as the sole reinforcement. With this material, 1m x 0.5m x 30 mm thick slabs were cast according to different procedures. Beam specimens, further tested in 4-point bending (4pb), have been sawn from them, in such a way that the direction of the principal tensile stresses resulted respectively parallel, transverse or randomly oriented with respect to the casting flow direction, along which fibers are likely to be aligned, thanks to the viscosity of the fluid mixture balanced at the purpose. From the undamaged portions of the tested beams, double edge notched square tiles were then obtained and tested according to a novel "Double-Edge Wedge Splitting" (DEWS) technique, which is deemed to provide the tensile stress-crack opening law, as an alternative to direct tension tests. The correlation between the thus identified law and the one obtained through inverse analysis from bending tests will be assessed, also in the sight of calibrating suitable crack opening limits for the definition of residual strengths. Furthermore, due to the above described specimen manufacturing process, quantitative correlation will be assessed between relevant material constitutive parameters, as above, and fiber orientation, suitably detected through image analysis.

1 INTRODUCTION

The ability of randomly dispersed discontinuous fibers to enhance the fracture toughness of brittle matrix, such as a cement based material, has been known for a long time, dating back to mud bricks reinforced with straw and horsehair in use in ancient Egypt.

Fiber reinforced concrete and cementitious composites actually represent the "up-to-date state of the art application" of this concept. All along an almost half a century odyssey, initiated by the pioneer studies by Romualdi & Batson (1963), the increase of knowledge about fiber reinforcing mechanisms, both in the field of theoretical modeling and experimental evidence, has led to continuous developments in new materials, processing techniques, standards and high end products for building structures and other civil engineering applications.

Nowadays a wide variety of fiber reinforced cement based composites is available, which are characterized by a range of engineering properties in terms of workability, mechanical strength and stiffness, fracture toughness and ductility, durability, fire and impact resistance, pricing and constructability, which may be selected depending on the specific application to be designed and built. As recognized by Naaman & Reinhardt (2006), among the most urgent issues to be tackled to promote increased structural applications of fiber reinforced cementitious composites, there is the need to specify different performance levels for their key engineering properties, together with the need to show how a particular fiber and fiber concrete mixture can lead to a prescribed level of performance.

As for the former issue, they have proposed to use as a key distinguishing material characteristic, whether the mechanical response of the composite to tensile loading is strain-hardening or strain-softening, and, in parallel, whether the structural behavior in bending is deflection-hardening or deflection-softening. "Conventional" deflection softening FRCs are well suitable for a wide range of applications, from the lower end represented by the control of plastic shrinkage cracking (Naaman et al. 2005, Banthia & Gupta, 2006) to the reduction/substitution of conventional reinforcement in concrete pavements and slabs on grade (Meda et al. 2006), to the higher end when fibers are, e.g., used to replace conventional shear reinforcement in precast prestressed elements (di Prisco & Ferrara, 2001). Deflection hardening composites, on the other hand, may be useful, if not necessary, when structural elements primarily subjected to bending have to be designed. This may lead to optimized shape and size of structural elements, with reduced self weights. This also results into a more rational design of the supporting structure and consequently yields to a

more time- and cost-effective construction process, including costs for transportation, erection, capacity of lifting equipments etc. As further bonuses, improvements e.g. in durability related properties are likely to be achieved, such as imperviousness, diffusion resistance etc., from which the structural performance all along the anticipated life cycle may surely benefit (Naaman, 2008).

Within this cutting-edge framework, precast construction industry may be regarded as the most straightforward recipient of related technology transfer, able and willing to put forward on the construction market elements and components for high end structural applications.

Naaman (1987) has demonstrated, by applying classical composite and fracture mechanics concepts, that a critical volume fraction of fibers is needed to obtain a strain-hardening behavior in tension or a deflection hardening behavior in bending. Such critical volumes depend, besides fiber aspect ratio, fiber-matrix bond and matrix cracking strength, also on the dispersion and orientation of the fibers with respect to the direction of the applied stress. The possibility of still keeping a deflection hardening behavior with a relatively low amount of fibers (*e.g.* around 1% by volume) is attractive from the cost point of view and may also simplify the material and structural manufacturing processes, thus opening the way to more widespread and larger scale practical applications. A reliable identification procedure of the tensile stress-crack opening relationship to be employed in design is needed to safely and sustainably promote such applications of HPFRCC

Very recent research (Ferrara et al. 2008, Stahli et al. 2008) has shown that the dispersion and orientation of fibers in concrete structural elements can be effectively controlled by a suitably balanced set of fresh state properties and a carefully designed casting procedure. The key idea of the whole process is that the fluid mixture must be first of all self compacting. This would allow to fill the formworks without any vibration or manual compaction, which may hinder homogeneous fiber dispersion and hence affect the final structural performance due to flaw effect of fiber-free or poorly reinforced zones. In details, the fresh state performance must be characterized by an adequate viscosity, to drive the fibers along the direction of the flow and orient them according to the fluid velocity field lines. The value of the yield stress must be also carefully calibrated, to control, within a reasonable range, the downward settlement of fibers due to their higher specific gravity with respect to the suspending fluid mortar. Furthermore, in order the final structural performance to fully benefit of this, the casting process must be carefully designed so to make the flow direction of fresh concrete, along which fibers may be aligned, to match as close as possible with the direction of the principal tensile stress within the structural element when in service. To pave the way for spreading such an approach into the design and manufacturing practice of HPFRCC precast structural elements, the effect of fiber orientation, as governed through the fresh state performance and the casting process, has to be assessed through a suitable experimental procedure. This should form an integral part of the design approach in order to identify material parameters which are meant as relevant to it.

This paper addresses the above said multifold issues with reference to a HPFRCC, containing 100 kg/m^3 straight steel fibers (l_f = 13 mm; d_f = 0.16 mm), designed for precast roof elements and slabs where fibers have to serve as the sole reinforcement (di Prisco et al. 2008).

1m x 0.5m slabs, 30 mm thick, as in the foreseen application, have been cast, according to different procedures. Beam specimens were then cut from hardened slabs and tested in 4-point bending. As it will be further explained, specimens were cut in such a way that the beam axis was oriented in different ways with respect to the direction of the concrete flow during casting. Since fibers tend to align along the direction of the concrete flow this allowed to obtain different orientation of fibers with respect to the tensile stress applied during 4pb tests, *i.e.* in the direction of the beam axis. double edge notched square tiles were then obtained from the undamaged portions of the tested specimens, and tested according to a novel “double-edge wedge splitting” technique (di Prisco et al. 2010), which is deemed to provide, as an alternative to direct tension tests, the tensile stress-crack opening law.

The correlation between the thus identified law and the one obtained through inverse analysis from bending tests will be assessed, also in the sight of calibrating suitable crack opening limits for the definition of residual strengths. Furthermore, due to the specimen manufacturing process, quantitative correlation will be assessed between relevant material constitutive parameters and fiber orientation. The non-secondary aim of the study is to show how to exploit the correlation among fresh state performance, fiber dispersion and hardened state properties of SCSFRCC to achieve a prescribed level of performance tailored to the specific application.

2 MIX-DESIGN AND FRESH STATE BEHAVIOR

Mix-design of the HPFRCC employed in the present investigationis shown in Table 1. A self-consolidating performance in the fresh state was sought and achieved, as witnessed by standard test results summarized in Table 2. The ability of the

mix to drive the fibers along its flow, guaranteeing their uniform dispersion and a tailored orientation within cast structural elements, was also checked. Dedicated tests, either in the fresh and hardened state, were performed as well as X-rays and image analysis of selected regions/cross sections of suitably manufactured specimens. Information about these issues can be found in (Ferrara et al. 2009, Ozyurt et al. 2009).

Table 1. Mix-design of HPFRCC employed in this study.

Constituent	quantity kg/m^3
Cement type I 52.5	600
Slag	500
Sand 0-2 mm	982
Water	200
Polycarboxilate SP	33 (lt/m^3)
Steel fibers (l_f/d_f = 13/0.16)	100

Table 2. Results of fresh state characterization tests.

Test (ref. standard)	Parameter	Measured value
Slump-flow	average diameter	755 mm
(UNI 11041)	Time to 500 mm T_{50}	4 seconds
V-funnel	flow time T_V	23 seconds
(UNI 11042)		
L-box	time to 200 mm t_{200}	2.5 seconds
(UNI 11043)	time to 400 mm t_{400}	4 seconds
height ratio	1	
U-box	height ratio	0.98
(UNI 11044)		
J-ring	constrained slump flow	750 mm
(UNI 11045)	diameter	

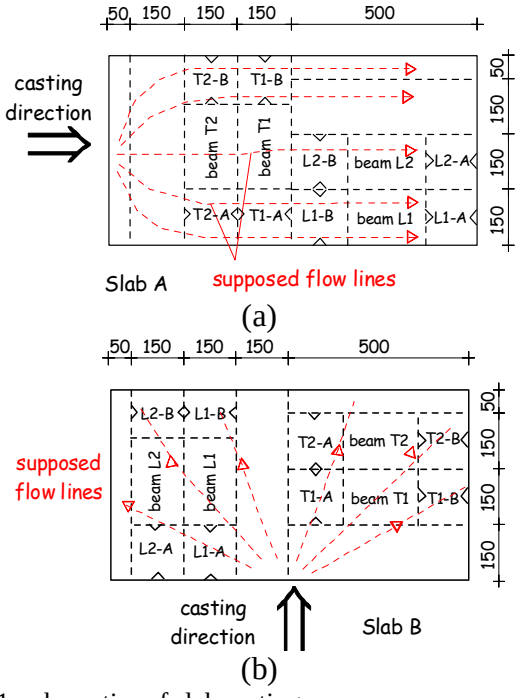

Figure 1. schematics of slab casting.

3 SPECIMEN "MANUFACTURING"

Moving from the concept and production of a construction material towards realizing the intended application, a crucial step stands in defining a sound and reliable procedure for the identification of relevant material properties which have to be employed in design calculations.

In the case of fiber reinforced cementitious composites, the identification of a "constitutive" stress crack-opening (or stress-strain) relationship is required, to be employed in the framework of dedicated design approaches and procedures. Several standards and guidelines (Italian CNR-DT204, RILEM TC162-TDF) are nowadays available to this purpose. Three or four point bending tests on prismatic notched specimens are recommened to obtain a (nominal) stress vs. crack (mouth or tip) opening displacement, from which the constitutive law to be employed in design has to be identified (di Prisco et al. 2004a). In the case of high performance fiber reinforced cementitious composites, which, thanks to a multicrack stable propagation stage can achieve a deflection hardening behavior, bending tests on unnotched prisms are recommended. Direct tensile tests on dog-bone or dumbbell specimens remain the most suitable, even if not easily performable, for strain hardening materials.

In the framework of this study, aimed at assessing the influence of flow-induced fiber orientation on the mechanical performance of the composite, 1m x 0.5m x 30 mm thick slabs were cast, according to "tailored" procedures, as schematically shown in Figure 1.

In one case, fiber reinforced material was poured at one of the shorter edges (Fig. 1a), allowing it to flow parallel to the longer sides. In the other (Fig. 1b), material was poured at the center of the longer edge, and formwork were filled by an almost radial spread of the fresh concrete.

Beam specimens 150 mm wide and 500 mm long were cut from the hardened slabs, according to the scheme also shown in Figure 1, and further tested in 4-point bending. In one case (Fig. 1a) it is evident the axis of the beams, and hence the direction of the principal tensile stresses due to the applied bending action, was either parallel (labeled as beam L in Fig. 1a) or perpendicular (beams labeled as beam T in Fig. 1a) to the flow direction of the fresh concrete, along which the fibers are believed to be aligned. In the other case (Fig. 1b), the coincidence is likely to be jeopardized by the radial flow, to an extent which is not easily a-priori quantifiable, unless through some Computational Fluid Dynamics modeling of the casting flow (Roussel et al. 2007). Four beams were cut from each slab. The remaining portions of the slabs (non-labeled in Fig. 1) were used to calibrate a non-destructive method to detect fiber dis-

persion based on capacitive and resistive properties of the fiber reinforced cementitious composite (Faifer et al. 2009).

After the tests, 150 mm side square tiles were sawn from the undamaged portions of each beam (i.e. the regions between the support and the load-point closest to it). A triangle cut and a notch were then grooved at two opposite edges (Fig. 2), in order to perform the newly conceived Double Edge Wedge Splitting Test, as described further in this paper (see also di Prisco et al. 2010). Also in this case specimen cutting and notch grooving were done in such a way that the most probable flow-induced orientation of fibers was either parallel (specimens labeled as B in Fig. 1) or perpendicular (specimens labeled as A in Fig. 1) to the tensile stresses induced during the tests (i.e. alternatively perpendicular or parallel to the notch-prearranged fracture plane).

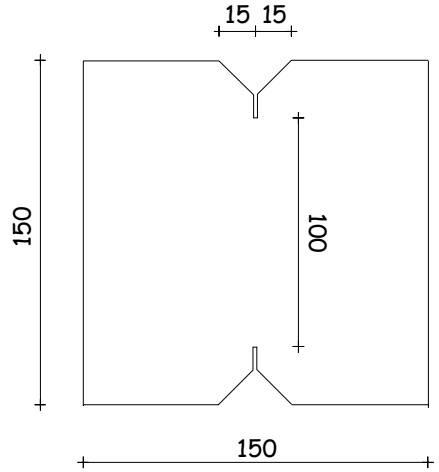

Figure 2. geometry of the specimen for Double Edge Wedge Splitting test (DEWS) – measures in mm.

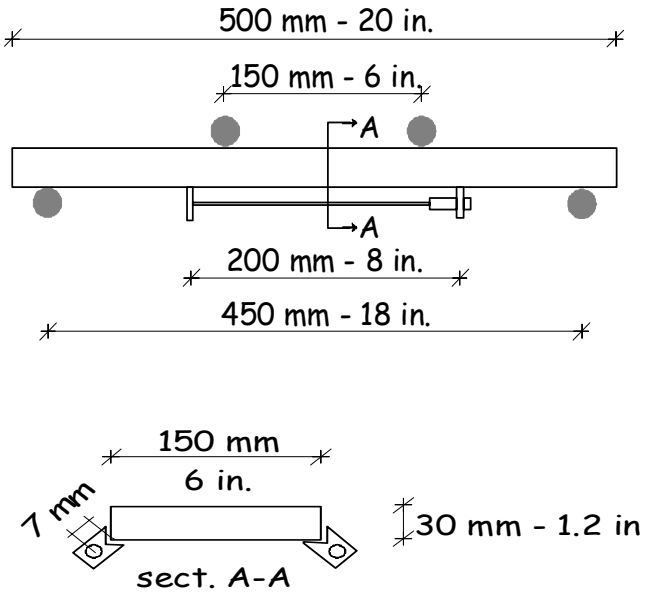

Figure 3. test set-up for 4pb tests.

4 EXPERIMENTAL TESTS AND RESULTS

4-point bending (4pb) and Double Edge Wedge Splitting (DEWS) tests were performed on specimens, manufactured as detailed in the previous section. As a whole, eight 4pb and sixteen DEWS tests were performed.

4.1 *4 point bending tests*

4-point bending tests were performed in displacement control according to the set-up shown in Figure 3. Since stable multi-cracking may be likely to occur in the constant bending moment region before localization into a single unstable propagating crack, crack opening displacement (COD) was taken as an integral measure over a 200 mm gauge length, astride the central region itself.

Nominal stress vs. COD curves (Fig. 4a-b) provide clear evidence of the effectiveness to align fibers along the flow direction of the fresh concrete, thanks to its suitably balanced viscosity, also as a function of the casting flow geometry. It also appears to what extent the thus tailored fiber orientation is able to influence the mechanical performance of the material in the hardened state.

In order to proceed with a quantitative analysis of the mechanical performance as above described, suitable indicators of the fracture toughness at different levels of crack opening have been calculated. Dealing with a deflection-hardening fiber reinforced material, the behavior of which is characterized by pre-peak multiple cracking followed by a single crack localization, the "processing" of the load-COD curve to the above said purpose must be handled with care. The different length scales involved in the have to be taken into account and guideline prescriptions have to be adequately modified. In the pre-peak regime, where multiple cracking has been observed in the central constant-bending-moment region of the specimens, the length-scale governing the measured load-COD behavior may be assumed equal to the COD-measuring gauge-length (ℓ_{COD} = 200 mm). On the other hand, once the localization into a single crack has occurred, the fracture governing length scale can be assumed equal to the specimen depth *h*. This does not apply to the case of beams cut from slab A in Figure 1a with the axis vertical to the flow (beams T1/2), for which a conventional-SFRC deflection-softening behavior was measured, with no multiple cracking. The governing length scale is equal to *h* all along the fracture process. In this case, coherently with a straightforward application of current Italian guidelines on the design of SFRC structures (CNR DT 204), from the nominal stress vs. COD curves the following stresses and equivalent post-cracking strengths have

been calculated as indicators of the material mechanical performance:

- the first cracking strength, f_{If}, defined as the maximum nominal stress in the COD range 0-0.1 mm, the corresponding COD being defined as w_I;
- the equivalent post-cracking strengths $f_{eq,1}$ and $f_{eq,2}$, defined as the nominal stress averaged in the COD range 3-5 w_I (0.3-0.5 mm) and 0.02h ± 20% (0.48-0.72 mm), the last one corresponding to an average tensile strain over the cross section equal to 1%. The aforementioned values are supposed representative of the material load-bearing capacity in SLS and ULS.

It is by the way worth remarking that for the very thin structural elements herein dealt with, the second COD range may prove inadequate for a correct design-oriented identification of a tensile stress vs. crack-opening law. This either because it partially overlaps with the first one and may be not enough representative of the ductility and deformation capacity of the material. For this reason post-cracking equivalent strength corresponding to a higher COD range, equal to 0.10h±20%, has been herein calculated, for a reliable identification of the tensile stress-crack opening law from bending tests.

Whenever a deflection-hardening behavior accompanied by pre-peak multiple cracking has been observed, the procedure for the calculation of equivalent post-cracking strengths was modified as follows:

- the peak nominal stress, $\sigma_{N,peak}$ and the corresponding strain $\varepsilon_{peak} = COD_{peak}/\ell_{COD}$ were calculated;
- the crack opening ranges for equivalent post-cracking strengths were redefined according to the following relationships:

- for $f_{eq,1}$ $(3\text{-}5\ w_I - \varepsilon_{peak}\ h) + \varepsilon_{peak}\ \ell_{COD}$ (1a)
- for $f_{eq,2}$ $(0.02h\pm20\% - \varepsilon_{peak}h) + \varepsilon_{peak}\ \ell_{COD}$ (1b)
- for further limits $(0.10h\pm20\% - \varepsilon_{peak}h) + \varepsilon_{peak}\ \ell_{COD}$ (1c)

Table 3. Results of 4pb tests (stresses in N/mm^2).

Specimen	f_{If}	$\sigma_{N,peak}$	$f_{eq,1}$	$f_{eq,2}$	$f_{eq,010h}$
Slab A					
L1	12.6	26.0	24.8	23.5	16.6
L2	15.4	27.6	26.7	24.6	12.2
T1	9.2	9.2	8.0	8.9	7.0
T2	8.9	8.9	8.4	8.8	6.8
Slab B					
L1	12.4	24.1	23.3	23.5	13.7
L2	12.7	23.5	22.9	21.4	15.2
T1	12.2	20.3	19.7	19.2	12.2
T2	11.7	19.4	19.4	18.9	13.5

These hypotheses result in post-cracking equivalent strengths that are representative for the same openings of the localized crack. The results are summarized in Table 3 for all the eight specimens tested in 4-point bending, providing detailed information for a thorough appreciation of the mechanical performance of the material.

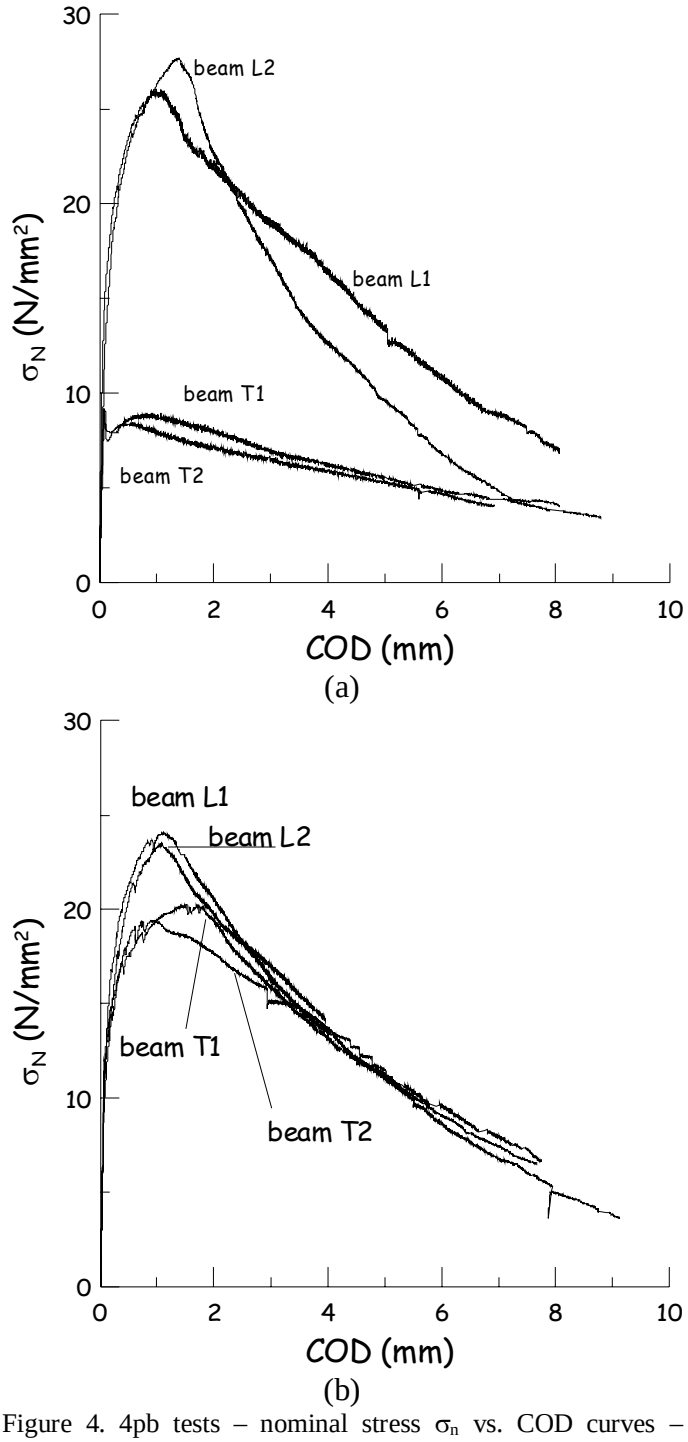

Figure 4. 4pb tests – nominal stress σ_n vs. COD curves – specimens cut from slab A (a) and from slab B (b).

4.2 *Double Edge Wedge Splitting tests*

Figure 5 shows a detail of the test set-up, together with the positioning of measuring instruments and a picture of the specimen under testing. Crack opening displacement was measured over a 50 mm length on

both sides of the specimen at three different positions along the ligament by means of LVDTs.

Tests were performed controlling the actuator displacement: the traction force acting on the ligament was calculated from the measured applied force also taking into due account the effects of friction (Fig. 6). The coefficient of friction was experimentally quantified by means of a dedicated test as explained in detail in a companion paper by di Prisco et al. (2010).

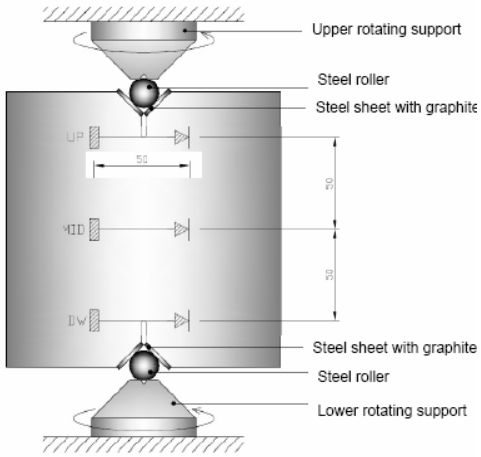

(a)

(b)

Figure 5. schematic of test set-up for DEWS tests (a) and picture of a specimen under testing (b).

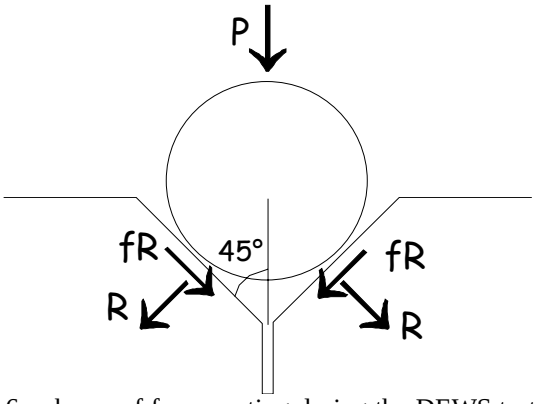

Figure 6. scheme of forces acting during the DEWS test: P applied force; R force on the ligament; fR friction force (f friction coefficient between steel rolled and sheets).

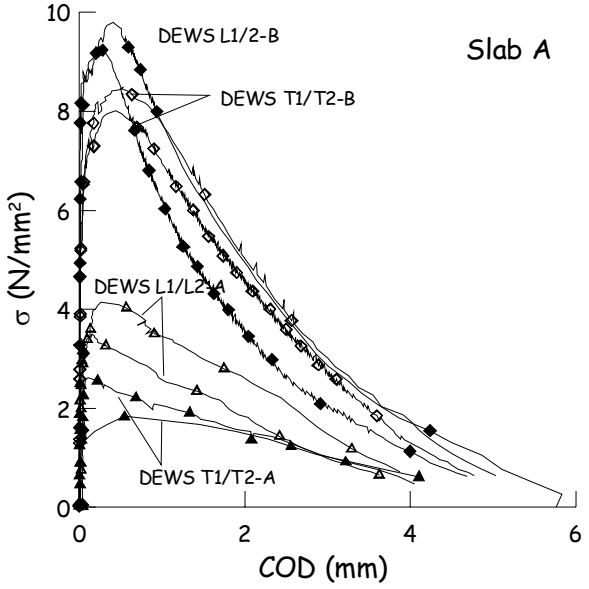

(a)

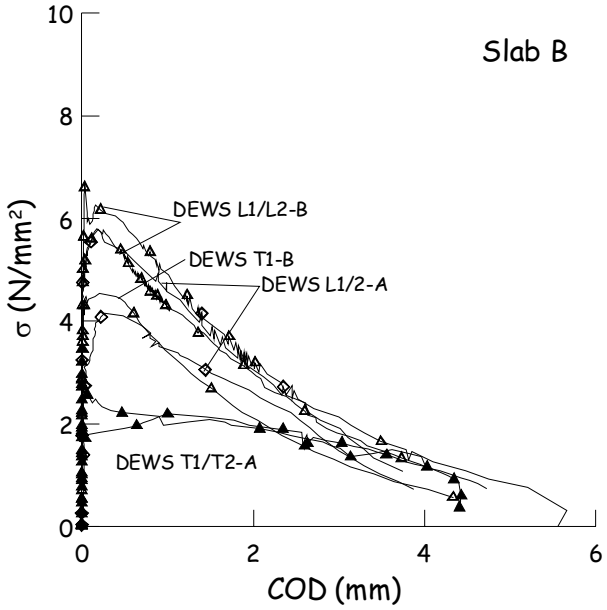

(b)

Figure 7. DEWS tests - stress vs. COD curves – specimens cut from slab A (a) and from slab B (b).

Figure 8. out of plane rotation of specimen B-T2A.

Figure 7 shows the results in terms of stress vs. average COD, which confirm the previous findings from 4pb tests about the effect of the flow induced fiber orientation on the mechanical properties of the composite. The poor performance of specimens B-T1B and B-T2B is due to a high out-of-plane rotation (Fig. 8- about 14° in both tests – see also di Prisco et al. 2004b). It is worth here remarking that such an out-of-plane rotation occurred in all specimens, but was always lower than 2°. Cracking always initiated on the side of the specimen corre-

sponding to the free surface during casting, which. most likely had a poorer fiber content due to their downward settlement.

A quantitative analysis of the measured performance has also been performed. Coherently with above referred Italian guidelines on the design of SFRC structures as well as with the proposed adaptations to the case of HPFRCC, the following stresses and post-cracking strengths were calculated:
- the first cracking strength, f_{If}, defined as the maximum nominal stress in the COD range 0-0.05 mm, the corresponding COD being defined as w_I;
- the peak stress, σ_{peak} and the corresponding strain $\varepsilon_{peak} = COD_{peak}/\ell_{COD}$ were calculated;
- the post-cracking strengths corresponding to the following crack opening ranges:

- for $f_{eq,1}$ $(3\text{-}5\ w_I - \varepsilon_{peak}\ h) + \varepsilon_{peak}\ \ell_{COD}$ (2a)

- for $f_{eq,2}$ $(0.01h \pm 20\% - \varepsilon_{peak} h) + \varepsilon_{peak}\ \ell_{COD}$ (2b)

- for further limits
$(0.05h \pm 20\% - \varepsilon_{peak} h) + \varepsilon_{peak}\ \ell_{COD}$ (2d)

The results are summarized in Table 4 for all the sixteen tested DEWS specimens.

Table 4. Results of DEWS tests (stresses in N/mm^2).

Specimen	f_{If}	$\sigma_{,peak}$	$f_{eq,1}$	$f_{eq,2}$	$f_{eq,005h}$
Slab A					
L1-A	3.0	4.2	4.1	3.8	1.9
L1-B	8.3	9.8	9.3	8.2	3.2
L2-A	3.2	3.5	3.2	3.0	1.3
L2-B	7.1	9.3	8.9	7.5	2.5
T1-A	1.8	3.6	1.8	1.9	1.8
T1-B	6.3	8.5	8.2	7.8	3.0
T2-A	1.8	2.6	2.0	2.1	1.6
T2-B	6.6	8.0	7.8	7.1	2.9
Slab B					
L1-A	3.0	4.2	4.1	3.8	1.9
L1-B	5.2	5.8	5.5	4.9	2.2
L2-A	5.2	5.5	5.5	5.1	2.4
L2-B	6.4	6.7	6.2	5.8	2.6
T1-A	2.4	2.5	2.3	1.8	1.2
T1-B	loss of control				
T2-A	2.2	2.6	2.5	2.1	1.3

5 "CONSTITUTIVE" BEHAVIOR: INFLUENCE OF FIBER ORIENTATION

To pave the way to structural applications made with the produced HPFRCC, the identification of "constitutive" stress-strain and/or stress crack opening relationships has to be pursued. The experimental data presented and discussed in the previous section, allow such a task to be performed either directly from DEWS tests or by means of inverse analysis from 4pb test results. This also enables to cross evaluate the reliability of both the experimental procedure based on the DEWS test and of the inverse analysis one from 4pb tests. For the latter, reference will be made to average values for each couple of nominally identical specimens (i.e. either L1-2 and T1-2 cut from both slabs), which showed a fairly limited scattering (Fig. 4a-b).

As a starting point reference has been made to the procedure recommended by the Italian guidelines (CNR DT 204), suitably modified to take into account the deflection hardening behavior. Coherently with another previous work by the authors (di Prisco et al. 2004a), it is proposed herein to consider:

- a pre-peak stress-strain law (Fig. 9a), in which the first linear elastic branch matches with CEB-Model Code prescriptions;

- a post-peak stress crack-opening law (Fig. 9b) which can be still identified as in CNR-DT204, by carrying out inverse analysis, also accounting for the pre-peak stress-strain law.

Besides the crack opening ranges defined in Equation (1a-b), to which the post-cracking equivalent strengths $f_{eq,1}$ and $f_{eq,2}$ correspond (Table 3), a further crack opening stage has been considered, at $w_u = 0.10h$ and the corresponding equivalent strength calculated in the range defined in Equation (1c). The σ-w laws shown with solid markers in Figures 10-11 are thus obtained. For beams T1/2 from slab A, which exhibited a deflection softening behavior, the pre-peak constitutive branch is meaningless.

In Figures 10-11 a-c the constitutive laws obtained as explained in the previous paragraphs are compared with those directly provided by the DEWS tests.

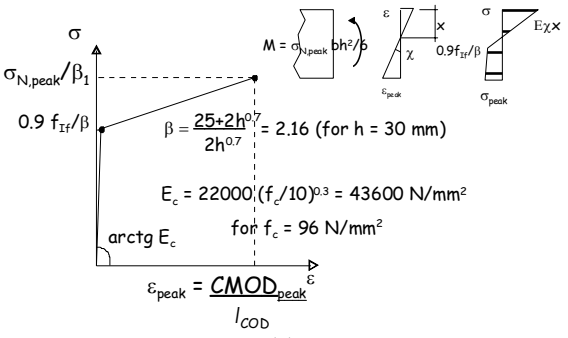

Figure 9. pre-peak stress-strain (a) and post-peak stress crack-opening (b) laws for deflection-hardening materials (coefficients $\beta 1$, $\kappa 1$ and $\kappa 2$ computed through inverse analysis).

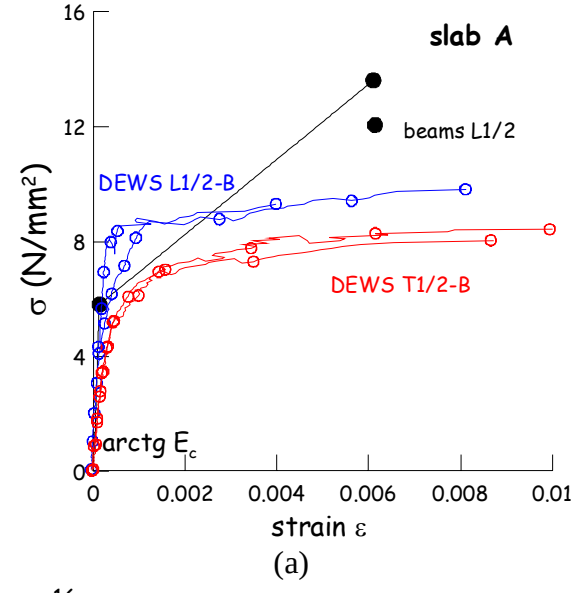

(a)

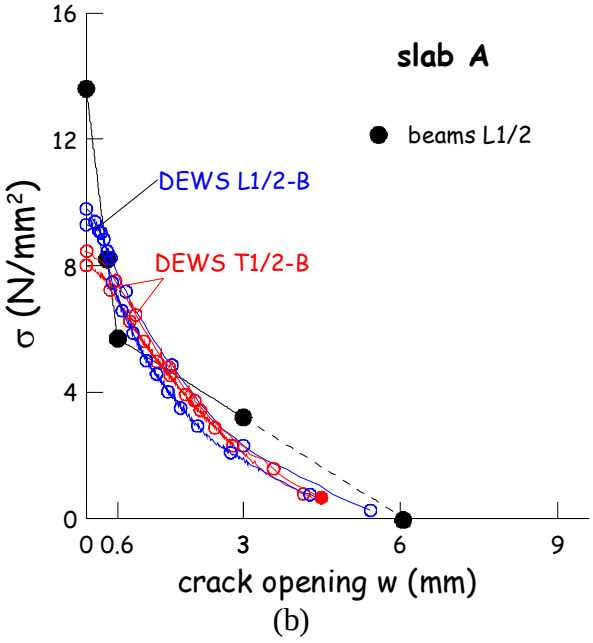

(b)

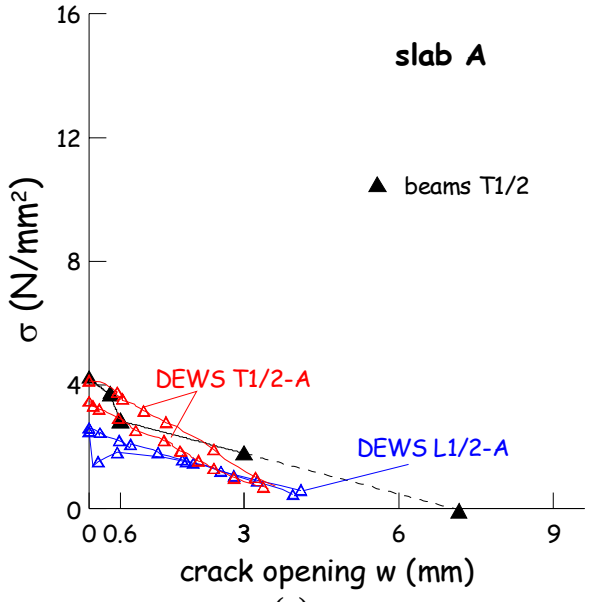

(c)

Figure 10. comparison between stress-strain/crack opening relationship identified from 4pb tests (inverse analysis) and experimental ones from DEWS tests: pre-peak behavior (a): post-peak with fibers parallel to tensile stresses (b) and fibers perpendicular to tensile stresses (c) (Slab A).

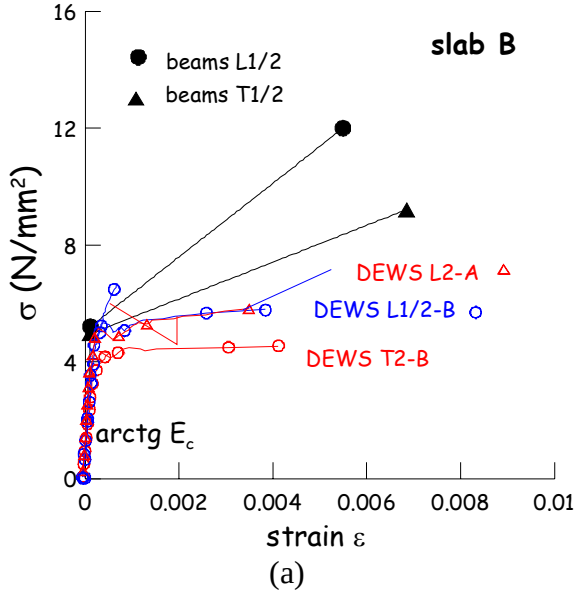

(a)

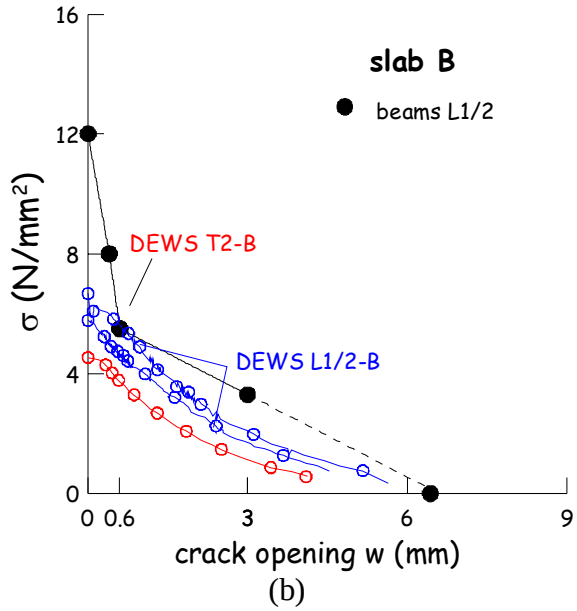

(b)

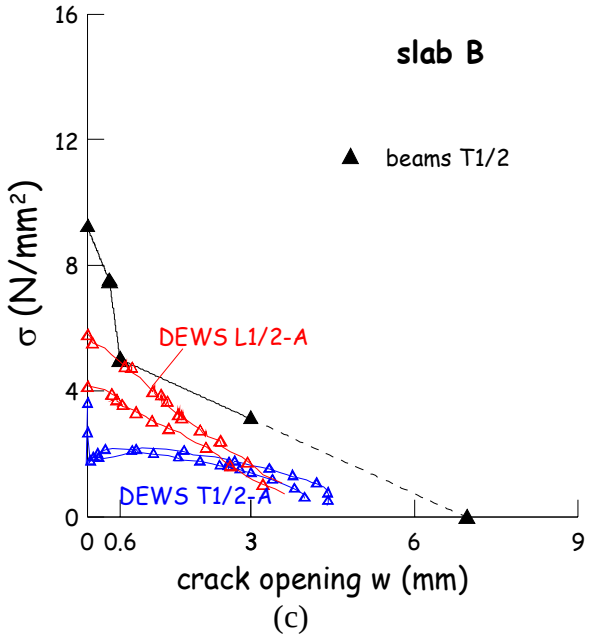

(c)

Figure 11. comparison between stress-strain/crack opening relationship identified from 4pb tests (inverse analysis) and experimental ones from DEWS tests: pre-peak behavior (a): post-peak with fibers parallel to tensile stresses (b) and fibers perpendicular to tensile stresses (c) (Slab B).

Comparison is made with reference to similar relative orientation of the fracture cross section to the casting flow direction and to the most probable orientation of fibers. The strain in the pre-peak branch of DEWS curves has been calculated dividing the average COD by the gauge length (50 mm).

The following issues are worth being highlighted:
- the pre-peak constitutive behavior identified from 4pb tests always shows a higher peak stress as well as a higher "hardening" modulus than in DEWS test results; this may be the outcome of a most likely downward settlement of fibers (see Ferrara et al. 2009), which acts favorably in the case of 4pb tests;
- except for very early softening stage, which may be affected by the above said differences in the pre-peak behavior, there is a remarkable agreement between the post-peak behavior as identified from 4pb and DEWS tests in most of the investigated cases, which refer to different fiber orientation with respect to the applied tensile stress.
- the value of the crack opening at zero stress identified by means of inverse analysis from 4pb tests, which is close to half the fiber length (l_f = 13 mm), is likely to be roughly confirmed also by DEWS test results.

The relatively good agreement detectable in Figures 10-11, besides supporting the reliability of the proposed experimental and identification procedures (di Prisco et al. 2004b), also allows to evaluate about the influence of the casting flow geometry on the random dispersion and tailored orientation of fibers. It appears that a good homogeneity of fiber dispersion almost all over the cast slab has been obtained in the case of slab A, where, after an initial transient flow where the fresh material is poured, formwork was filled by an almost unidirectional flow parallel to the longer edges of the slab. In the case of slab B, where a radial flow of fresh concrete filled the moulds, the direction of fibers, as induced by the fresh concrete flow, was different in each of the tested specimens, thus justifying the larger differences between results from 4pb and DEWS tests, mainly in the case of beams T1/2 and related DEWS specimens (e.g. in slab B, unlike in slab A, specimen DEWS T2B differ from DEWS L1/2B).

These statements, which provide a physical interpretation of the measured and identified behavior of the material, need further quantitative confirmation (Soroushian and Lee, 1990; Stroeven, 2009).

In a previous work (Ferrara et al. 2009), the authors performed, for 4pb specimens, a refined image analysis to identify fiber orientation parameters on the fracture cross sections. Calculated fiber orientation densities for the analyzed specimen surfaces are shown in Figure 12. The fiber orientation density may be correlated to the total fiber projected length in the given direction, expressed in probabilistic terms.

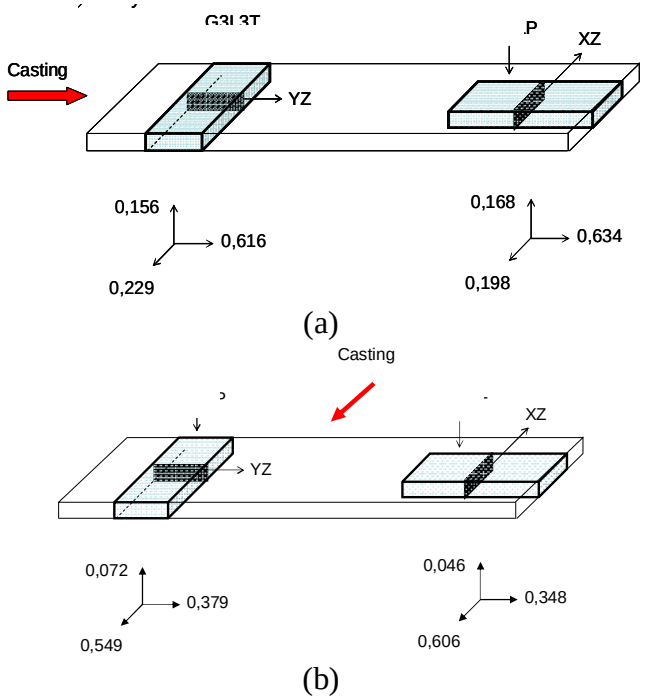

Figure 12. fiber orientation densities on fracture surfaces of selected 4pb specimens from slab A (a) and slab B (b).

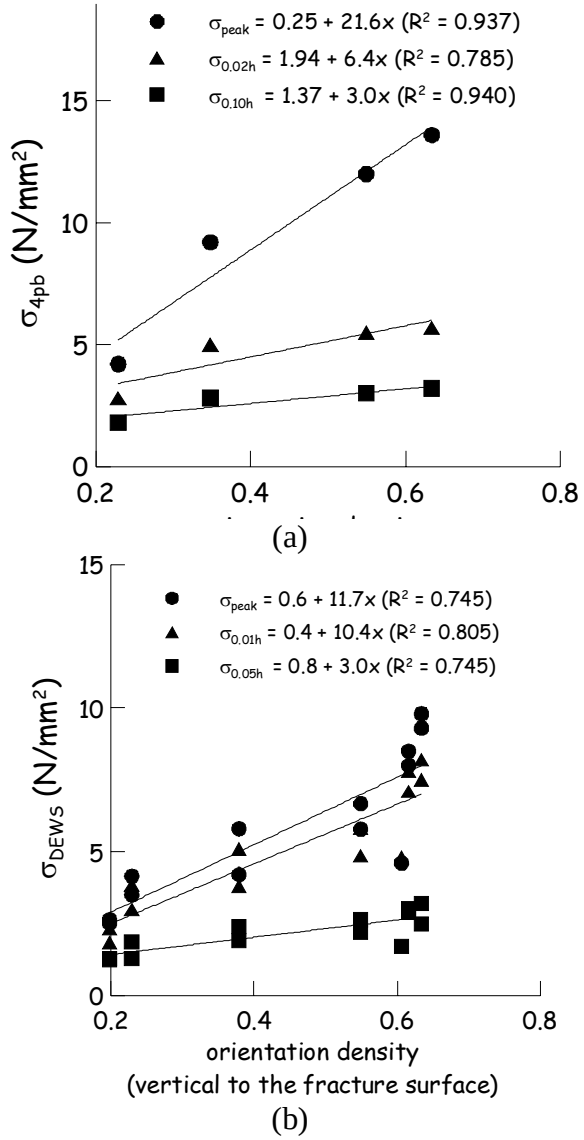

Figure 13. influence of fiber orientation on stresses at different crack openings calculated from 4pb tests (a) and DEWs tests(b).

Results of this analysis were correlated to the measured values of the equivalent post-cracking nominal strengths, showing their strong dependence on the "fiber orientation density" vertical to the fracture surface. Such a strong correlation is also confirmed by Figure 13a, where the values of the "true stress" at different crack openings as identified by means of inverse analysis have been plot vs. the fiber orientation density vertical to the fracture surface. In Figure 13b the same correlation has been sought for stresses experimentally identified from DEWS test results, by hypothesizing that the same fiber orientation densities as for 4pb specimens features their cross sections, as detailed in Figure 12. Despite some larger scattering, which is likely due to the assumption of retaining throughout the slabs the same orientation densities as for the analyzed fracture cross sections of 4pb beams, the relevant characteristics of the identified trend appear to be confirmed, thus providing further evidence to the reliability of either the identification procedure employed for 4pb tests and the novel experimental technique.

6 CONCLUSIONS AND FURTHER WORK

The influence of fiber orientation, as driven by the casting flow of fresh concrete thanks to its balanced fresh state performance, on the mechanical behavior of High Performance Fiber Reinforced Cementitious Composite has been analyzed in this study. A suitably "tailored" procedure has been employed to the purpose. Casting process and specimen geometry have been designed so to have a wide range of flow induced fiber orientations, which were characterized by means of image analysis in a separate study. Mechanical performance was experimentally investigated by means of either 4-point bending tests on unnotched beams and by a newly developed technique, named Double Edge Wedge Splitting Test. This has been shown to provide directly the tensile constitutive behavior of the HPFRC, in good agreement with the one identified from 4pb tests by means of inverse analysis, where fracture toughness up to higher crack opening limits has been considered due to the high material performance. This provided interesting evidence on the reliability of the proposed new experimental test and identification procedure. The possibility to achieve, through to the fresh state properties of the mixture and a carefully designed casting process, a "tailored" orientation of fibers and thus control the mechanical performance of the material, has also been assessed.

REFERENCES

Banthia, N. & Gupta, R. : "Influence of polypropylene fiber geometry on plastic shrinkage cracking in concrete", Cem. and Concr. Res., 36 (7), 2006, 1263-1267

CNR-DT204: "Guidelines for the design, manufacturing and control of SFRC structures", 2006, (in Italian).

di Prisco, M. & Ferrara L.: "HPFRC pre-stressed thin-web elements: some results on shear resistance", Proc. FraMCoS4, Cachan (France), 2001, R. de Borst et al. eds., Balkema, 895-902

di Prisco, M., Ferrara, L., Colombo, M. & Mauri, M.: "On the identification of SFRC costitutive law in uniaxial tension" in Fiber reinforced concrete, Proc. BEFIB 04, di Prisco M. et al. eds., 2004a, 827-836.

di Prisco, M., Felicetti, R., Lamperti M. & Menotti, G.: "On size effect in tension of SFRC thin plates", Proc. FraMCoS 5, V.C. Li et al., (Eds.), 2, B.L. Schmick & A.D. Pollington, USA, 2004b, 1075-1082.

di Prisco, M., Lamperti, M.G.L., Lapolla & S., Khurana, R.S. "HPFRCC thin plates for precast roofing", Proc. 2nd Intl. Symp. on HPC, Kassel, 2008, 675-682.

di Prisco, M., Lamperti, M.G.L. & Lapolla, S.: "On Double Edge Wedge Splitting test: preliminary results", submitted for publication to Framcos 2010.

Faifer, M., Ottoboni, R., Toscani, S., Ferrara, L. & Felicetti, R.: "A multi-electrodes measurement system for steel fiber reinforced concrete materials monitoring", Proc. IMTC09, IEEE Conf., Singapore, 2009, 313 -318.

Ferrara, L., Park, Y.D. & Shah, S.P.: "Correlation among fresh state behaviour, fiber dispersion and toughness properties of SFRCs", ASCE J. Mat. Civ. Eng., 20 (7), 2008, 493-501.

Ferrara, L., Ozyurt, N. & di Prisco, M.: "High mechanical performance of fiber reinforced cementitious composites: the role of "casting-flow" induced fiber orientation", *accepted for publication on Materials & Structures, January 2010.*

Meda, A., Plizzari G.A. & Riva, P.: "Fracture behaviour of SFRC slabs on grade", Materials and Structures, 37 (6), 2004, 405-411.

Naaman, A.E.: "High Performance Fiber Reinforced Cement Composites", Proc. IABSE Symp. on Concrete Structures for the Future, Paris, France, 1987, 371-376.

Naaman, A.E.: "Development and evolution of tensile strain hardening FRC composites", in Design and Application, in Fiber reinforced concrete , Proc. BEFIB 2008, RILEM PRO 60, Chennai, India, R. Gettu ed., , Rilem Pubs., 2008, 1-28.

Naaman, A.E., & Reinhardt, H.W.: Proposed classification of HPFRC composites based on their tensile response", Materials and Structures, 39 (5), 2006, 547-555.

Naaman, A.E. Wongtanakitcharoen, T. & Hauser, G.: "Influence of different fibers on plastic shrinkage cracking of concrete", ACI Materials Journal, 102 (1), 2005, 49-58.

Ozyurt, N., Tregger, N., Ferrara, L., Sedan, I. & Shah, S.P.: "Adapting fresh state properties of fiber reinforced cementitious material for high performance thin-section elements", Proc. Rheo-Iceland, O. Wallevik et al. eds., 2009, 313-321.

RILEM TC-162-TDF Test and design methods for steel fiber reinforced concrete. Mat. and Struct., vol. 33, 2000, 75-81.

Romualdi, J.P. & Batson G.B.: "Mechanics of crack arrest in concrete", ASCE J. Eng. Mechs., 89, (3), 1963, 147-168.

Soroushian, P. & Lee, C.D.: "Distribution and orientation of fibers in steel fiber reinforced concrete", ACI Materials Journal, 87 (5), 1990 433-439.

Roussel, N., Geiker, M.R., Dufour, F., Thrane, L.N. & Szabo, P.: "Computational modelling of concrete flow: general overview" , Cem. and Concr. Res., 37, 2007, 1298-1307.

Stahli, P., Custer, R. & van Mier, J.G.M.: "On flow properties, fibre distribution, fibre orientation and flexural behaviour of FRC", Mat. & Struct., 41 (1), 2008, 189-196.

Stroeven, P.: "Stereological principles of spatial modeling applied to steel fiber reinforced concrete in tension, ACI Materials Journal, 106 (3), 2009, pp. 213-222.